DYNAMIC ANALYSIS OF A ROTOR SYSTEM BASED ON MOTORIZED SPINDLE THERMAL CHARACTERISTICS

Zinan WANG[1, 3] , Ke ZHANG[1,3], Gheorghe OANCEA[2, 3], Xiaotian BAI [1,3 *], Tianxiao ZHANG[1] and Zhipeng WU[1]

[1]*School of Mechanical Engineering, Shenyang Jianzhu University, Shenyang, 110168, China*
[2]*Department of Manufacturing Engineering, Transilvania University of Brasov, Brasov, 500036, Romania*
[3]*Joint International Research Laboratory of Modern Construction Engineering Equipment and Technology, Shenyang, Liaoning, 110168, China*
**e-mail: acetyws@163.com*

ABSTRACT*: In this paper, the motorized spindle temperature prediction model is established to analyze the temperature field. The thermal displacement of the bearing is calculated by using a simulation. Considering the thermal displacement of the bearing, the dynamic performance of angular contact bearing is solved based on the quasi-static research method. At the same time, the finite element model of motorized spindle rotor system is set up to analyze the bearing dynamic stiffness influence of motorized spindle dynamic characteristics. The accuracy of the model was verified by temperature rise of motorized spindle and modal experiments. The results show that with the increasing of rotating speed, the temperature of motorized spindle increases in a nonlinearly mode. In this paper, coupling analysis of thermal and dynamic characteristics of the spindle is conducted, it provides theoretical basis for the design and optimization of the spindle.*

KEYWORDS*: motorized spindle, thermal displacement, temperature field, dynamic stiffness, dynamic characteristics*

1 INTRODUCTION

It is well known that the motorized spindle uses a relatively closed structure and the operation of the spindle at a higher speed will generate a lot of heat. The heat generation is not easy to spread out. The temperature distribution inside the spindle is also very uneven. The thermal displacement makes the motorized spindle bearing stiffness and other parameters influence the dynamic characteristics of motorized spindle (Yuzhong & Yusuf, 2004; Sun et al. 2018, Chang, 2019).

Du et al. proposed a spindle symmetrical solution for the thermal error problem based on the thermal behavior analysis to reduce thermal error, but the dynamic properties are ignored (Du et al. 2015). Another research group analyzed the relationship between thermal deformation and vibration based on the finite element method and thermal analysis, but the effect of bearing on spindle is not studied (Lee at al, 2015). Hwang and Kim proposed a method that is able to determine the optimal bearing preload and estimate the equilibrium temperature by considering the spindle speed and bearing loads, but the shaft of the motorized spindle system was neglected (Hawang & Kim 2015, Kim et al. 2015). In other research is proposed a thermal network spindle model based on the fractal and Hertz contact theory to analyze the whole thermal deformations of the motorized spindle system, but the distribution of thermal field was not researched (Liu et al. 2015). Although Kudoyarov, Zinov and Basharov studied the adaptive control of motorized spindle in a multifunctional machine tool to improve effective operation, the effect of the bearing is not deeply studied (Kudoyarov et al. 2016). Shatokhin and Golovin developed motorized spindles with axial spindle oscillations to increase the tool life in the grinding, however the dynamic shaft stiffness of the bearing was not considered (Shatokhin & Golovin, 2016) Some researchers calculated the dynamic models to predict the system at high speed ranges, but the influence of the bearing thermal displacement is neglected (Shaik & Srinivas, 2014; Sathiya & Prabhu, 2014; Xul et al. 2017).

Most of the above researches are focused on the dynamic thermal characteristics or thermal state characteristics of motorized spindle, while ignoring the coupling relationship between dynamic characteristics and thermal state characteristics of motorized spindle. Having in view the above studies, in this paper is presented how is established a temperature field model of the spindle and obtained the temperature of the motorized spindle at different speeds.

The thermal displacement of the bearing is solved by using the simulated temperature method. Meanwhile, considering the thermal displacement of the bearing, the dynamic stiffness of the bearing and the dynamic characteristics of the motorized spindle are analyzed. The influence of temperature rise of motorized spindle on its dynamic characteristics is obtained, which provides data support for spindle design.

2 DYNAMIC CHARACTERISTIC MODEL OF BEARING THERMAL DISPLACEMENT

2.1 The temperature field of finite element motorized spindle boundary condition model calculation

In this paper, it is assumed that all losses are converted into heat, that is, the generated heat of the motor is equal to the loss P. The loss P of the motor is composed of eddy current loss P_e, hysteresis loss P_h, electrical loss P_{cu} and mechanical loss P_n (Kudoyarov et al. 2016). The calculation of each loss is shown in the following equation (Zheng D. & Chen W, 2017):

$$\begin{cases} P_e = \sigma_e (Bf)^2 \\ P_h = \sigma_h f B^2 \\ P_{cu} = \sum I_x^2 R_x \\ P_n = \pi C \rho \omega^3 R^4 L \end{cases} \quad (1)$$

where: σ_e - the constants of material specifications and performance, B - the amplitude of flux density, f - the frequency of flux change, σ_h - material coefficient, I_x - the current in the x winding, R_x - the resistance of the x winding is converted to the reference working temperature, π - the friction coefficient is determined by experience, r - air density, ω - the angular velocity, R - outer radius of rotor, L - the length of rotor

Using Palmgren's empirical formula, the calculation method of bearing heat generating Q is shown in the equation (Li et al. 2016):

$$Q = 1.047 \times 10^{-4} nM \quad (2)$$

where: Q - the heat of bearing, n - the rotation speed of the motorized spindle, M - moment of bearing friction.

The value of moment is the sum of bearing viscous friction moment M_0 and load moment M_1. The expression of viscous friction moment M_0 is (Sathiya & Prabhu, 2014):

$$M_0 = 10^{-7} f_0 (v_0 n)^{2/3} d_m^3, \quad v_0 n \geq 2000 \quad (3)$$

The expression of load moment M_1 (Chen et al.):

$$M_1 = Z (F_s / C_s)^y (0.9 F_a \operatorname{ctg} \alpha - 0.1 F_r) d_m \quad (4)$$

where: v_0 - viscosity of lubricant, d_m - pitch diameter of bearing, F_s - equivalent static load(N), C_s - nominal static load, Z and y - the experimental coefficients of bearing design.

The internal heat transfer behavior of the motorized spindle includes heat transfer between the shaft end and the air, heat transfer between rotor and air gap, heat transfer between the bearing and the compressed air, heat transfer between stator and cooling water, the natural heat transfer between surface of the shaft and the air. The calculation methods of each heat transfer coefficient are shown in Table 1.

Table 1 Heat transfer coefficient calculation method of spindle

Position of heat exchange	Calculation method	Influencing factor
The end of shaft	$h_1 = 28(1+\sqrt{0.4}$	u - circumferential velocity of rotor (m/s)
Bearing	$h_2 = c_0 + c_1 u^{c_2}$	c_0, c_1, c_2 respectively 9.7, 5.33, 0.8. u is the average velocity through the bearing air (m/s)
The channel of cooling water	$h_3 = N_u \lambda_w / D$	N_u - Nusselt number of fluids, ω - The thermal conductivity of water(W/(m·℃)
Air gap	$h_4 = Nu \lambda_a / H$	λ_a - the thermal conductivity of air, H - qualitative dimensions of air gap
The surface of shaft	$h_5 = 9.7$	h_5 - heat transfer coefficient between the outer surface of the motorized spindle and the surrounding air

2.2 Temperature field model of motorized spindle

The model of motorized spindle is 150MD30Y10.The front bearing is 7007C and the rear bearing is 7006C.

When calculating the thermal deformation of bearing parts, Harris method is adopted. The relative axial and radial thermal displacement of the bearing inner and outer ring raceway calculation method is shown in equation 5 (Chen &Hsu, 2003):

$$\begin{cases} u_a = \frac{1}{2} \alpha_s (\Delta T_s L_s - \Delta T_h L_h) \\ u_r = \alpha_i \Delta T_i d_i [\alpha_s \Delta T_s (1+\mu_s) - \alpha_i \Delta T_i] - \alpha_h \Delta T_h (1+\mu_h) d_e \end{cases} \quad (5)$$

where: u_a,u_r - axial and radial relative thermal displacement of bearing inner and outer raceway, α_i - thermal expansion coefficient of bearing inner ring, T_i - bearing inner ring temperature rise, d_i - diameter of inner ring raceway, α_s - coefficient of expansion of shaft, α_h - thermal expansion coefficient of bearing, T_s - temperature rise of the rotor, T_h - temperature rise of the bearing housing, μ_s, μ_h - Poisson ratio of rotating shaft and bearing, d_e - diameter of outer ring raceway, L_s - length of shaft, L_h - length of bearing housing

The dynamic characteristics of bearings can be calculated by nonlinear equations including geometric equation, deformation equation, balance equation of ball etc. (Sayah et al. 2018)

The angular contact bearing of the motorized spindle which the inner ring and the curvature center of the outer ring raceway is unchanged. According to Fig. 1, the thermal displacement of the bearing ring is included, the axial distance A_{1j} and radial distance A_{2j} of the new inner ring and the outer ring curvature center are expressed by equation 6:

$$\begin{cases} A_{1j} = BD_b \sin\alpha_0 + \delta_a + \theta R_i \cos\varphi_j + u_a \\ A_{2j} = BD_b \cos\alpha_0 + \delta_r \cos\varphi_j + u_r \end{cases} \quad (6)$$

where: φ_j - the azimuth , φ_j=2p（j-1）/Z，j=1、2...Z，Z the number of balls, B=f_i+f_e-1，f_i, f_e - radius coefficient of raceway curvature, α - initial contact angle, δ_α - axial displacement of bearing under stress, δ_r - radial displacement of bearing under stress, θ - angle of bearing rotation under stress, R_i - center of curvature radius, D_b - diameter of ball.

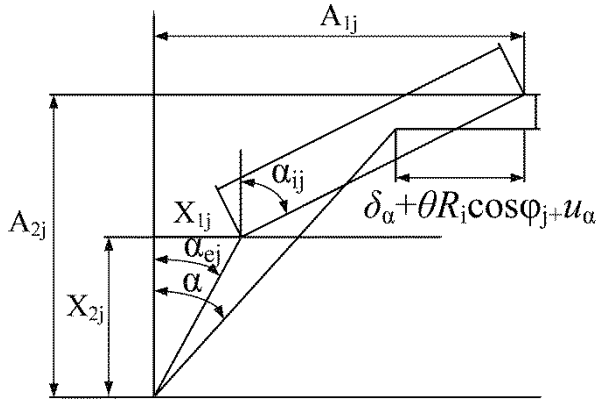

Fig. 1. Center position of bearing ball

The deformation equation can be obtained as shown in equation 7.

$$\begin{cases} \{A_{1j} - [(f_e - 0.5)D_b + \sin\alpha_{ej}\}^2 + \{[(f_i - 0.5)D_b + \delta_{ij}]\cos\alpha_{ij}\}^2 \\ - [(f_i - 0.5)D_b + \delta_{ij}]^2 = 0 \\ \{[(f_e - 0.5)D_b + \delta_{ej}]\sin\alpha_{ej}\}^2 + \{A_{2j} - [(f_i - 0.5)D_b + \sin\alpha_{ij}\}^2 \\ - [(f_e - 0.5)D_b + \delta_{ej}]^2 = 0 \end{cases} \quad (7)$$

Where δ_{ij},δ_{ej} are the contact ball deformations of inner and outer rings. When the bearing ball is rotating, it is subjected to the combined action of centrifugal force, gyroscopic moment and contact load, which the bearing force at the azimuth φ_j angle is shown in equation 8.

$$\begin{cases} Q_{ij}\sin\alpha_{ij} - Q_{ej}\sin\alpha_{ej} + 2\dfrac{M_{gj}\cos\alpha_{ej}}{D_b} = 0 \\ Q_{ij}\cos\alpha_{ij} - Q_{ej}\cos\alpha_{ej} - 2\dfrac{M_{gj}\sin\alpha_{ej}}{D_b} + F_{cj} = 0 \end{cases} \quad (8)$$

where: Q_{ij} - contact load of bearing ball and inner ring, Q_{ej} - contact load of bearing ball and outer ring, F_{cj} - centrifugal force of ball, M_{gj} - gyroscopic moment.

The bearing is subjected to axial preloading and radial loading, and the force balance equation of the bearing inner ring is shown in:

$$\begin{cases} F_a - \sum_{j=1}^{N} Q_{ij}\sin\alpha_{ij} = 0 \\ F_r - \sum_{j=1}^{N} Q_{ij}\cos\alpha_{ij}\cos\varphi_j = 0 \\ M - \sum_{j=1}^{N} Q_{ij}\sin\alpha_{ij} R_i\cos\varphi_j = 0 \end{cases} \quad (9)$$

where: F_a - axial load of bearing, F_r - Radial load of bearing, M - bending moment of bearing. During the operation of the motorized spindle, the radial support stiffness of the bearing calculation method is shown below:

$$K_r = \sum_{j=1}^{z} \frac{K_{rej}K_{rij}}{K_{rej} + K_{rij}}\cos^2\frac{2\pi}{Z}(j-1) \quad (10)$$

where: K_r - support stiffness of bearing, K_{rej} - radial contact stiffness component of ball and outer ring and K_{rij} - radial contact stiffness component of ball and inner ring.

2.3 Dynamic modeling of rotor system

The model of motorized spindle is 150MD30Y10.When establishing the finite element model of its dynamic characteristics, the motorized spindle shell, stator and other fixed parts are ignored. The rotor and rotating shaft are assumed to be a whole part. Every angular contact bearing is simplified to a spring with the same stiffness as the bearing.

3 ANALYSIS OF DYNAMIC CHARACTERISTIC SPINDLE BASED ON BEARING THERMAL DISPLACEMENT

3.1 Steady state temperature field of motorized spindle

The temperature inside the motorized spindle is very uneven. Since the rotor is located inside the motorized spindle, which is unfavorable to heat dissipation, and the stator is close to the cooling channel, most of its heat is taken away by cooling water. Although the stator generates heat twice as much as the rotor, its temperature is lower than that of the rotor. In the bearing structure, the friction between the bearing ball and the inner, outer ring occurs at the same time, so its temperature is the highest. The outer ring of the bearing is close to the cooling water, and its temperature is the lowest in the bearing structure. The variation trend of the front and rear bearing temperature at different speeds is shown in Fig. 2.

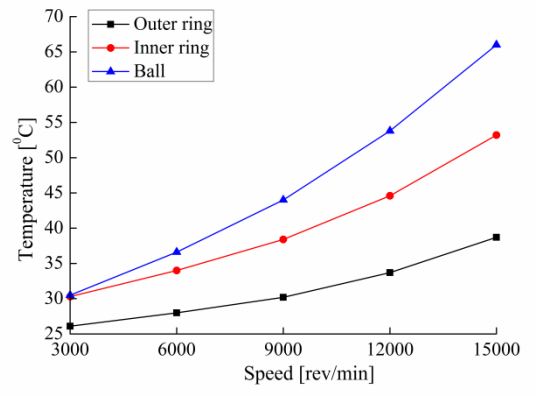

a) front bearing

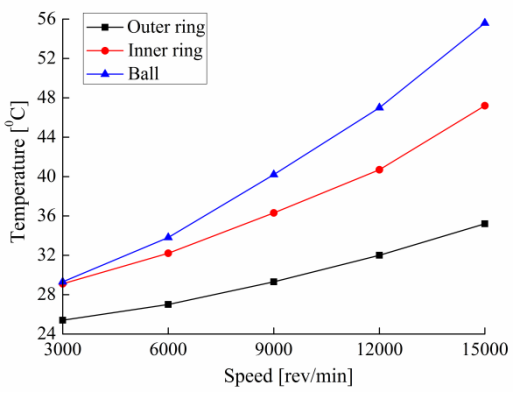

b) rear bearing

Fig. 2. Front and rear bearing temperature at different speeds

It can be seen in Fig. 2 that with the increase of rotating speed, the temperature rise of the bearing is non-linear, and the growth rate is faster and faster. As the ball diameter of the front bearing is larger than that of the rear bearing and the front bearing is close to the rotor, so the heat generation rate of the front bearing is higher.

3.2 Analysis of dynamic stiffness based on thermal displacement bearings

When the thermal displacement of the bearing ring is included, the variation trend of the radial bearing support stiffness with the rotation speed is shown in Fig. 3.

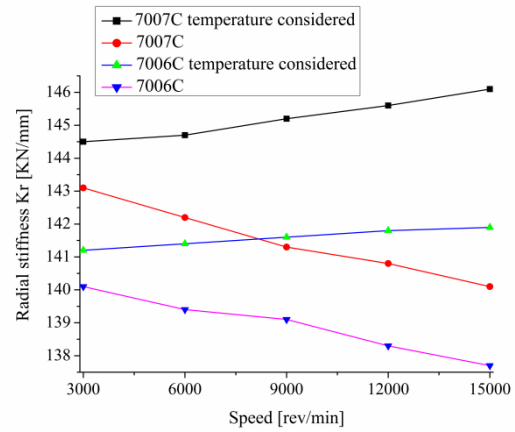

Fig. 3. Relationship between bearing stiffness and speed

According to the Fig. 3, in the motorized spindle system, the front bearing stiffness is relatively large under the same conditions. Without considering the thermal displacement of the bearing, under the combined action of contact load increase between the ball and the outer ring, the radial stiffness of the bearing decreases with the rotation speed increasing. Since the ball mass of the front bearing is large, the centrifugal force and gyro torque it bears are large, so the stiffness declines rapidly. As the rotation speed increases, the stiffness of the front bearing decreases by 1.6[KN/mm] and the stiffness of rear bearing decreases by 3[KN/mm]. However, after considering the thermal displacement of the bearing, with the contact load between the bearing ball and the inner, outer ring of the bearing increasing, the stiffness of bearing is larger. With the increase of rotating speed, the thermal displacement of the bearing and the stiffness of the bearing is increasing. When the rotation speed increases from 3000[rev/min] to 15000[rev/min], the stiffness of rear bearing is increased by 0.7[KN/mm] and the stiffness of front bearing is increased by 2.4[KN/mm].

3.3 Analysis of motorized spindle dynamic characteristics

The change of bearing support stiffness directly affects the motorized spindle dynamic characteristics. When considering the thermal

displacement of the bearing, the relationship between the natural frequency and the rotational speed of the motorized spindle is shown in Figure 4. It can be seen from Fig. 4 that the change trend of motorized spindle natural frequency is consistent with the change trend of bearing stiffness. When the thermal displacement of bearing is not included, with the increase of rotating speed, the natural frequency of motorized spindle is decreasing. When bearing thermal displacement is included, with bearing support stiffness increases the natural frequency of motorized spindle increases gradually. According to the above analysis, when the thermal displacement of the bearing is taken into account, the dynamic characteristics of the motorized spindle change significantly. Therefore, the influence of bearing thermal displacement cannot be ignored when analyzing the dynamic characteristics of motorized spindle.

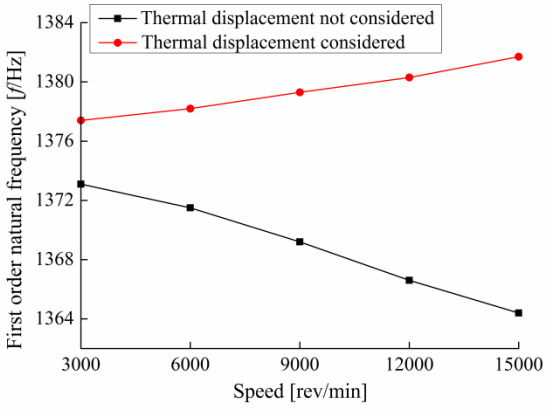

Fig. 4. Relationship between natural frequency and speed

4 TEMPERATURE AND MODAL EXPERIMENTS OF MOTORIZED SPINDLE

4.1 Temperature experiment of motorized spindle

As is shown in Fig. 5, 150MD30Y10 motorized spindle is tested. The experimental equipment include frequency converter, working table, TC-2008 multi-channel temperature tester, data acquisition system and other high-speed motorized spindle auxiliary analysis equipment.

The temperature is 20℃, the motorized spindle runs for 60 minutes without load at each rotation speed. The temperature sensor is used to measure the temperature of the spindle front bearing and the rear bearing. Compared with corresponding positions in the simulation model, The comparison results of steady temperature rise and transient temperature rise are shown in Fig. 6(a) and (b).

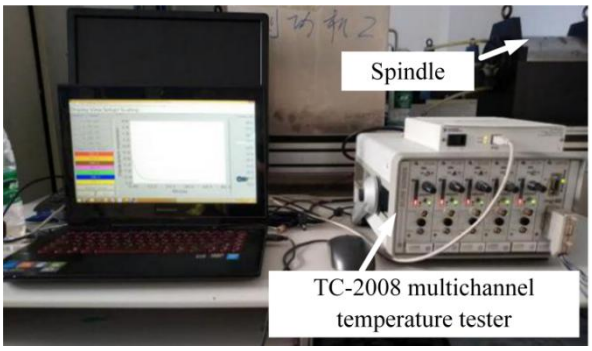

Fig. 5 Temperature test table of motorized spindle

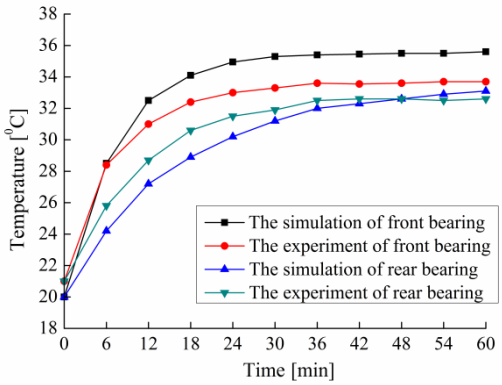

a) Comparison of transient state temperature experiment and simulation

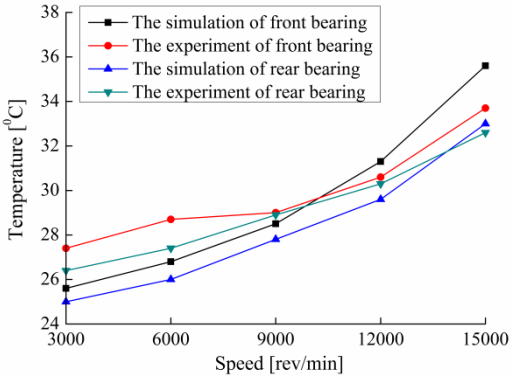

b) Comparison of steady state temperature experiment and simulation under different rotating speed

Fig. 6 Comparison of motorized spindle temperature field experiment and simulation

According to the Fig. 6(a), at the condition of 15000 [rev/min], the temperature rise speed of motorized spindle decreases with time, the temperature field of motorized spindle reaches equilibrium at 24[min]. The simulation results of motorized spindle transient temperature field are consistent with the experimental results. According to the Fig. 6 (b), the error between simulation results and experimental results is less than 10% for the steady-state temperature of motorized spindle at

different rotating speeds. Thus the thermal model of motorized spindle is more accurate.

4.2 Modal experiment of motorized spindle

When frequency converter provides frequency is close to the natural frequency of the system, it will cause resonance phenomenon, reduce the stability and processing quality of the machine. According to n=60f, the determination of the motorized spindle natural frequency is significant to predict the ultimate speed of spindle.

In this research, the natural frequency of motorized spindle is measured by a hammering method. When calibrating the natural frequency of the rotor system, LC0101 velocity sensor is placed on the motorized spindle shaft. Using SA-LE5K impact hammer hits the spindle which is shown in Fig. 7(a). The exciting force signal is processed by INV306DF intelligent signal analyzer. In order to ensure the accuracy of the measurement results, the sensor position and hammer position are changed for many times. The natural frequency response signals of the rotor system are obtained, as is shown in Fig. 7.

(a) Hammer test of natural frequency

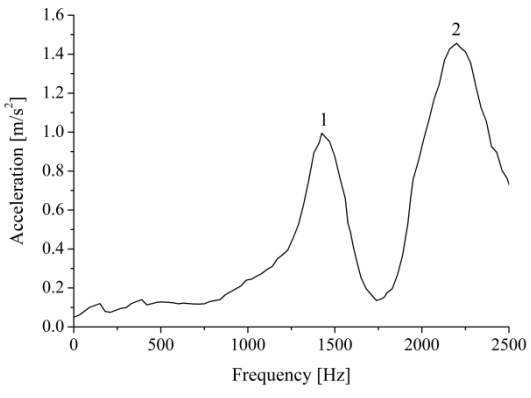

(b) Frequency domain analysis

Fig. 7. Response signal of hammer

According to the Fig. 7, the maximum error between the experimental value and the simulation value occurs in the second order natural frequency, the maximum error is 11.8%. The first-order natural frequency error is only 3.5%, and all the errors are controlled within 15%. It can be concluded that the finite element model is accurate and can truly reflect the dynamic characteristics of the motorized spindle, which can be used for variable parameters calculation.

5 CONCLUSION

In this paper, the temperature field of motorized spindle is simulated and modeled. The steady-state temperature of motorized spindle at different speeds is obtained and the dynamic stiffness of bearing, including thermal displacement and the dynamic characteristics of the motorized spindle, are analyzed. The paper reaches the following main conclusions:

a) As the motorized spindle speed increases, the temperature of motorized spindle is linearly increased. In the spindle structure, the rotor temperature which rises rapidly is higher than the stator temperature. In the bearing structure, the ball has the highest temperature and the fastest temperature rise.

b) Without considering the thermal displacement of the bearing, the stiffness of bearing occur softening phenomenon. After considering the thermal displacement of the bearing, the stiffness of bearing is compensated. Bearing stiffness is larger with the increase of rotation speed.

c) The first-order natural frequency of rotating shaft including bearing thermal displacement is higher than that of motorized spindle without displacement. And with motorized spindle speed increasing, the natural frequency of motorized spindle is gradually increased.

6 ACKNOWLEDGEMENT

This work was supported by the National Natural Science Foundation of China [Grant numbers 51675353, 51705341 and 51805337], The innovation team project about the Ministry of Education of China.[Grant number IRT-15R45], Doctor Start-up Foundation of Liaoning Province [Grant number 20170520147]

7 REFERENCES

[1] Cao, Y.Z. and Yusuf, A., (2004) A General Method for the Modeling of Spindle-Bearing Systems, *Journal of Mechanical Design*, 126,1089-1104.

[2] Chang, G. (2019). Rotor vibration feature recognition based on particle swarm optimization. *Academic Journal of Manufacturing Engineering,17*, 145-152.

[3] Sun, J, Wu, Y. H., Zhou, P., Wang, H., Zhang, K., Z, Li, S. H., and Yao J.M. (2018). Analysis of surface

morphology and roughness on SI3N4 ceramic gringing. *Academic Journal of Manufacturing Engineering*,16, 20-28.

[4] Du, Z. C. , Yao, S. Y., and Yang, J. G. . (2015). Thermal behavior analysis and thermal error compensation for motorized spindle of machine tools. *International Journal of Precision Engineering and Manufacturing, 16*(7), 1571-1581.

[5] Lee, J. , Kim, D. H. , and Lee, C. M. . (2015). A study on the thermal characteristics and experiments of high-speed spindle for machine tools. *International Journal of Precision Engineering and Manufacturing, 16*(2), 293-299.

[6] Hwang, Y. K. , and Lee, C. M., (2015). Development of a simple determination method of variable preloads for high speed spindles in machine tools. *International Journal of Precision Engineering and Manufacturing, 16*(1), 127-134.

[7] Kim, K. S. , Lee, D. W. , Lee, S. M. , Lee, S. J. , and Hwang, J. H. . (2015). A numerical approach to determine the frictional torque and temperature of an angular contact ball bearing in a spindle system. *International Journal of Precision Engineering and Manufacturing, 16*(1), 135-142.

[8] Liu, Z. , Pan, M. , Zhang, A. , Zhao, Y. , Yang, Y. , and Ma, C. . (2015). Thermal characteristic analysis of high-speed motorized spindle system based on thermal contact resistance and thermal-conduction resistance. *The International Journal of Advanced Manufacturing Technology, 76*(9-12), 1913-1926.

[9] Kudoyarov, R. G. , Zinov, V. L. , and Basharov, R. R. . (2016). Design and operation of the motorized spindle in a multifunctional machine tool. *Russian Engineering Research, 36*(2), 134-137.

8 [10] ZHENG, D. X., AND CHEN, W. F . (2017). THERMAL PERFORMANCES ON ANGULAR CONTACT BALL BEARING OF HIGH-SPEED SPINDLE CONSIDERING STRUCTURAL CONSTRAINTS UNDER OIL-AIR LUBRICATION. *TRIBOLOGY INTERNATIONAL, 109*, 593-601.

[11] Shatokhin, S. N. , and Golovin, A. O. (2016). Ultrasonic motorized spindle with hydrostatic bearings. *Russian Engineering Research, 36*(8), 692-695.

[12] Shaik, J. H., and Srinivas, J. (2014). Dynamic stability of a motorized high speed machine tool spindle supported on bearings. *Applied Mechanics and Materials, 612*, 29-34.

[13] Sathiya Moorthy, R., and Prabhu Raja, V. (2014). An improved analytical model for prediction of heat generation in angular contact ball bearing. *Arabian Journal for Science and Engineering, 39*(11), 8111-8119.

[14] Chen, X. , Liu, J. , He, Y. , Zhang, P. and Shan, W., (2013). Thermal properties of high speed motorized spindle and their effects. *Journal of Mechanical Engineering, 49*, 135-142.

[15] Xul, J. , Zheng, X. , Zhang, J. , and Liu, X. . (2017). Vibration characteristics of unbalance response for motorized spindle system. *Procedia Engineering, 174*, 331-340.

[16] Elhaj A. I. Ahmed, and Li S. S. (2019). Optimization of factors affecting vibration characteristics of unbalance response for machine motorized spindle using response surface method. *Mathematical Problems in Engineering*, (2), 1-12.

[17] Li S. S., Shen Y. and He Q. (2016). Study of the thermal influence on the dynamic characterstics of the motorized spindle system. *Advanced in Manufacturing* vol.4, 1-8

[18] Chen J. and Hsu W. Y. (2003). Characterizations and models for the thermal growth of a motorized high speed spindle. *International Journal of Machine Tools & Manufacture*, vol.43, 1163-1170

[19] Xi, S. T. , Cao, H. R. , and Chen, X. F. (2019). Dynamic modeling of spindle bearing system and vibration response investigation. *Mechanical Systems and Signal Processing, 114*, 486-511.

[20] Bai, X. T. , Wu, Y. H. , Zhang, K. , Chen, C. Z. , and Yan, H. P. . (2017). Radiation noise of the bearing applied to the ceramic motorized spindle based on the sub-source decomposition method. *Journal of Sound and Vibration, 410*, 35-48.

[21] Sayah, M. , Farouk, B. & Kaddour, R. (2018) The dynamic behavior of a rotary turbocharg supported by defective bearings, *Academic Journal of Manufacturing Engineering*,16,154-160

Data Availability

The data used to support the findings of this study are available from the corresponding author upon request.

Conflicts of Interest

The authors declare that they have no conflicts of interest